Ad Hoc Networks 119 (2021) 102540

Contents lists available at ScienceDirect

Ad Hoc Networks

journal homepage: www.elsevier.com/locate/adhoc

ADAPT: An Adaptive Directional Antenna Protocol for medium access control in Terahertz communication networks

Daniel Morales *, Josep M. Jornet

Department of Electrical and Computer Engineering, Northeastern University, United States

ARTICLE INFO

Keywords:
Terahertz
Medium access control
Directional networks
WLAN
6G

ABSTRACT

Terahertz (THz)-band (0.1–10 THz) communication is envisioned as a key technology for the next generation of wireless communications, with the potential to enable Terabit-per-second (Tbps) links. To overcome the high path loss of this band, the use of directional antennas on both transmitter and receiver is necessary even for distances of few meters. This paper presents an Adaptive Directional Antenna Protocol for THz networks (ADAPT), a novel medium access control (MAC) protocol tailored to ultra-high-speed directional networks in a centralized architecture. An access point with a turning antenna divides the space in sectors, and synchronization is achieved with a 3-way receiver-initiated handshake. The protocol implements adaptive sector time and modulation mechanisms. An analytical model to study the stability condition and achievable throughput is presented. The performance of ADAPT is investigated with extensive simulations in *ns-3* in terms of throughput and discard rate, using the physical layer defined in IEEE 802.15.3d, the first standard for THz communications. Results show that the proposed solution improves the current protocols and achieves throughput in excess of 100 Gigabit-per-second (Gbps), while reducing latency and packet discard rate.

1. Introduction

Today's society creates, shares and consumes information at an unprecedented rate, and expects high speed wireless connectivity *anywhere*, *anytime*. Terahertz (THz)-band (0.1–10 THz) communication is envisioned as a key wireless technology in beyond-5G communication systems [1], with the potential to meet the future demand for Terabit-per-second (Tbps) wireless data rates.

Laying between millimeter-wave and the far infrared, the THz band is one of the least explored bands of the electromagnetic spectrum. For years, it has been overlooked due to the lack of compact signal sources and detectors that efficiently operate at THz frequencies. However, the THz technology gap is quickly closing thanks to major recent advancements in several device technologies. On the one hand, approaching the THz band from the microwave and millimeter wave perspective, the limits of standard silicon CMOS, Silicon Germanium BiCMOS, as well as III–V semiconductor transistor and diode technologies are being pushed to their limits to reach the 1 THz mark [2–4]. On the other hand, when approaching the THz band from visible and infrared end of the spectrum, quantum cascade lasers, optical down-conversion systems and photo-conductive antennas are being explored [5,6]. Moreover, the unprecedented physical properties of new nanomaterials such as graphene [7,8], have been predicted to enable a new generation of wireless devices that intrinsically operate in the THz band [9]. All these technologies, whether individually or through hybrid combinations, are making the THz band a strong candidate for 6G systems and beyond.

The very large available bandwidth in the THz band, from tens of GHz up to a few THz, alleviates spectrum scarcity and enables ultra-high-speed physical data rates of hundreds of Gigabit-per-second (Gbps) [10]. At macro-scale distances, THz communication will enable applications such as Tbps WLAN, ultra-broadband outdoor backhaul networks and enhanced security in wireless networks. The small size of THz devices will also enable a new class of nano-scale applications.

Nonetheless, the low transmission power of THz transceivers and the high path loss, resulting from spreading and molecular absorption, introduce several challenges. Focusing in the macro-scale scenario, the use of highly directional antennas (DAs) is required both in the transmitter and receiver, in order to achieve link distances of several meters. Using DAs helps overcome the path loss by providing more gain, but creates a *deafness problem*, as neighbor nodes cannot communicate when their antennas are not facing each other. This is a new constraint for neighbor discovery and link-layer synchronization, which have traditionally relied on the use of omni-directional antennas. Another challenge is that of making an efficient use of the channel. When transmitting at hundreds of Gbps or even Tbps, the packet propagation delay can be in the same order of magnitude as the packet transmission time, making propagation time a limiting factor.

* Corresponding author.
E-mail address: morales.da@northeastern.edu (D. Morales).

https://doi.org/10.1016/j.adhoc.2021.102540
Received 10 December 2020; Received in revised form 9 March 2021; Accepted 4 May 2021
Available online 11 May 2021

There is a need to design a new medium access control (MAC) protocol tailored to the characteristics of the THz band. As discussed in Section 2, MAC protocols designed for lower frequencies cannot be reused, as the use of omni-directional antennas in at least one of the two ends would severely limit the range of communication.

In this paper, we present ADAPT, an Adaptive Directional Antenna Protocol for THz networks. This is a MAC protocol for ultra-high-speed centralized networks at macro-scale distances, where both the Access Point (AP) and the client nodes use narrow-beam DAs. The protocol relies on a turning AP that divides the space into sectors, periodically providing coverage to the whole area, and on a 3-way receiver-initiated handshake for link-layer synchronization and collision avoidance. The electronic beam steering capability of the AP can be realized with dense antenna arrays technology. Adaptive sector time and adaptive modulation mechanisms reduce cycle time and maximize the performance of the protocol. A 1-way handshake variant with reduced control overhead is also presented.

ADAPT is evaluated both analytically and with simulations in *ns-3*. We present an analytical model that studies the stability condition and achievable throughput. In *ns-3*, the protocol is implemented using *TeraSim* [11], an extension that models the frequency-selective channel and physical layers of the THz band. The performance is investigated in terms of throughput and packet discard rate with extensive simulations, using the physical layer parameters of the IEEE 802.15.3d standard. It is compared to a non-adaptive version of the 1-way handshake protocol, and to Carrier Sense Multiple Access with and without collision avoidance (CSMA, CSMA/CA).

The remainder of this paper is organized as follows. In Section 2 we summarize the related works. The THz system model used is explained in Section 3. The protocol design is presented in Section 4, and an analytical model in Section 5. In Section 6 we present and discuss the results obtained. Finally, Sections 7 and 8 summarize future work and conclusions.

2. Related works

For the time being, research in the THz band has focused mainly on devices, the channel and the physical layer. Networking solutions are still quite unexplored and only a few MAC protocols tailored to THz networks have been proposed.

The millimeter wave (mmWave) band (30 GHz–300 GHz) is the closest to THz. MAC protocols in IEEE 802.11ad [12] and IEEE 802.11ay [13], for communication networks at 60 GHz, also use directional antennas. However, the characteristics of mmWave and THz communications are significantly different. At 60 GHz, with lower path losses, a meaningful range can be achieved with omni-to-directional (O-to-D) antenna pairs, while directional-to-directional (D-to-D) links are required at THz. Moreover, bandwidth at mmWave is narrower, and physical data rates are much slower. In 802.11ad, 2.16 GHz wide channels are used, compared to the several tens to hundreds of GHz of continuous bandwidth available in the THz band. Overall, the proposed MAC protocols for mmWave cannot be reused in THz networks.

As for MAC design in the THz band, few protocols have been proposed so far. A comprehensive survey on MAC for THz networks [14] gathers all the proposed protocols to date, including both macro-scale and nano-scale scenarios. Focusing on the solutions for macro-scale centralized architectures, we can classify the few proposed protocols by the strategy used to achieve link-layer synchronization, the main challenge in highly directional networks.

2.1. Dual-band approach

As proposed in [15,16], a possible approach is to use two radios, one operating at sub-6 GHz frequencies for control packets, and another for fast data transmissions employing directional THz links. The benefit of sub-6 GHz is the fact that omni-directional antennas can be used without compromising distance. After establishing synchronization using omni-to-omni (O-to-O) antenna pairs in a sub-6 GHz channel, nodes would switch to the THz radio for ultra-high-speed data transfers in a D-to-D link.

While this is a feasible solution, it requires at least two radios. Using a radio at sub-6 GHz would also defeat the purpose of alleviating spectrum scarcity of lower bands. Moreover, the slower data rate of control signals may introduce a too large overhead time for high speed networks.

2.2. Use of omni-directional antennas

Omni-directional communication at THz frequencies is used in [17] for link establishment and synchronization, where control packets are exchanged using an O-to-D antenna pair in a THz channel. After synchronization, D-to-D links are used for data transmission, thus enabling the use of more complex modulations and higher data rates.

Nevertheless, with the current and foreseeable transmission power of THz transceivers, the use of even one omni-directional antenna severely limits the range of communication. Only D-to-D antenna pairs provide enough gain to achieve distances of several meters.

2.3. Receiver-initiated handshake

The use of a turning AP and a receiver-initiated handshake is proposed in [18] for a centralized network architecture. Beam steering enables the AP to periodically sweep an area divided in sectors. When turning into a new sector, it sends a Clear-To-Send (CTS) packet that indicates availability to receive. Client nodes are directionally listening to the AP, and can only transmit data after receiving a CTS. All packets are sent on D-to-D links at THz, avoiding the use of multiple radios and not compromising range with omni-directional communication. This solution successfully works around the deafness problem and provides link-layer synchronization.

However, the AP uses a fixed sector time, leading to a low channel utilization. In addition, the collision avoidance mechanism employed is not reliable, as carrier sensing also suffers from the deafness problem.

This paper takes the approach of a receiver-initiated handshake, presented in [18], as we recognize its potential to overcome the deafness issue and establish synchronization while only using D-to-D links that do not compromise range. The protocol proposed in this paper solves the problems of low channel utilization and unreliable collision avoidance, achieving up to a ten-fold increase in throughput and an effectively null packet discard rate.

2.4. On neighbor discovery

One of the most critical challenges of THz networks is that of neighbor discovery. Directional beams, while necessary, create a deafness problem that makes locating nearby nodes becomes a complex task. Literature that tackle this challenge is scarce, but some techniques have been proposed recently, such as single-shot discovery using leaky antennas [19], or expedited neighbor discovery by leveraging the side lobes [20]. We are aware of this obstacle and propose a possible approach, in Section 4.4, that has synergies with the protocol presented.

3. THz system model

3.1. Network architecture

We design a protocol for a centralized architecture in macro-scale networks. It is governed by a central AP that provides connectivity to client nodes, which are randomly distributed in a two-dimensional plane. The AP coordinates all transmissions, maximizing efficiency and guaranteeing fairness. In this paper, only up-link communication is defined and analyzed, but the protocol can be extended to include down-link. This type of architecture is relevant for WPAN, WLAN or small cells in beyond-5G/6G cellular networks.

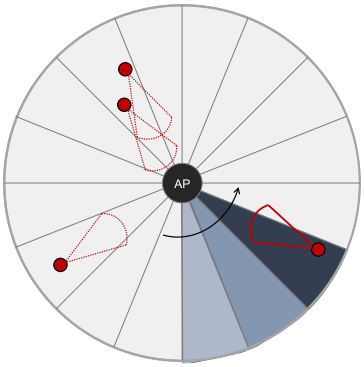

Fig. 1. Network architecture: A central turning AP divides space in sectors, and nodes are randomly distributed in a 2-D plane.

3.2. Turning directional access point

We assume that nodes and AP are equipped with dense antenna arrays that support dynamic beamforming and beam steering [21–23]. With these capabilities, we define a turning AP that divides space in sectors by discretizing the antenna azimuth, as in Fig. 1. We assume that nodes have already discovered the AP and are always directionally listening towards it. When the AP turns into a sector, it will initiate the handshake by sending a Call-to-Action (CTA) packet, which can trigger a data transmission. We consider that communication occurs only in line-of-sight (LOS) D-to-D links. We do not take into account multi-path propagation, as THz communications rely mainly on LOS due to the very high attenuation that non-LOS signals suffer. Nonetheless, if the LOS path was blocked and a node discovered the AP through a reflective surface, using another sector, it would make no difference from a MAC design perspective.

3.3. Terahertz channel

The high path loss is the most important constraint in THz macro-scale communications. The propagation of electromagnetic waves is mainly affected by two phenomena, namely, spreading and molecular absorption. Based on the channel model in [24], the channel frequency response is defined as

$$H_c(f,d) = \left(\frac{c}{4\pi f d}\right) \exp\left(-\frac{k_{\text{abs}}(f)\, d}{2}\right), \tag{1}$$

where f stands for frequency, d for distance, c refers to the speed of light and k_{abs} to the molecular absorption coefficient of the medium. With this frequency response, power at reception P_r is given by

$$P_r(d) = \int_B S_t(f)\, |H_c(f,d)|^2\, G_t\, G_r\, df, \tag{2}$$

where S_t is the single-sided power spectral density of the transmitted signal, B is the bandwidth and G_t, G_r are the gain of the transmitter and receiver antennas, respectively.

Noise also has two components, thermal and molecular absorption noise. However, if signals are transmitted in absorption-defined windows, we can neglect the effect of molecular absorption on noise. We will consider only thermal noise, calculated as

$$N = k_B\, T\, B, \tag{3}$$

where k_B is the Boltzmann constant, T is temperature and B is bandwidth. It is important to note that, since thermal noise depends on bandwidth, ultra-broadband communications in the THz band will have very high noise values. For reference, at 75 GHz of bandwidth and 300 K of temperature, thermal noise is of −65 dBm.

Table 1
Sectors, Beamwidth and gain relation.

N_{sec}	Beamwidth ($\Delta\theta$)	Max. Gain [dB]
15	24°	18.55
20	18°	21.04
30	12°	24.57
45	8°	28.09
60	6°	30.59
90	4°	34.11
120	3°	36.61

3.4. Range/performance trade-off

The AP beamwidth chosen plays a key role in the performance and range of the network. A narrower beamwidth leads to more gain and longer range, but also results in a larger number of sectors, slowing the turning speed and effectively worsening the overall protocol performance.

Beamwidth ($\Delta\theta$) is defined as the beam angle overture for which the gain is at most 3 dB weaker than the maximum gain. Each AP full cycle is divided into a number of even sectors (N_{sec}), given by

$$N_{\text{sec}} = \frac{2\pi}{\Delta\theta}. \tag{4}$$

The antenna gain is inversely proportional to the beam effective area. For highly directional antennas, the gain can be approximated as [25]

$$G \approx \frac{4\pi}{\Omega_A} = \frac{4\pi}{\theta_h \phi_h}, \tag{5}$$

where Ω_A is the array solid beam angle, and θ_h and ϕ_h refer to the half power beam width (HPBW) in the elevation and azimuthal plane respectively. We will assume an identical angle in both planes, so that $\Delta\theta = \theta_h = \phi_h$. We also consider that nodes and AP use the same beamwidth, so $G = G_t = G_r$. The relation between number of sectors, beamwidth and gain is captured in Table 1.

In order to properly decode a signal, P_r must be high enough to satisfy the Signal-to-Noise-Ratio threshold (SNR_{th}). We can use Eq. (2) to calculate the necessary gain to achieve a certain distance, and adjust beamwidth accordingly. Nonetheless, a high number of sectors is detrimental to the protocol performance, as it will increase cycle time. Moreover, with a longer range comes an increase in propagation time, which is a limiting factor in THz networks. Therefore, a compromise has to be made to find an optimal balance between range and network performance.

4. Protocol design

In this section, we present and discuss the design of ADAPT. A variant of the protocol using a 1-way handshake is also proposed. We conclude with a note on neighbor discovery.

4.1. 3-way handshake and adaptive sector time

The most challenging question in directional networks is that of overcoming the deafness problem. In ADAPT, we rely on a turning AP and a receiver-initiated handshake to establish link-layer synchronization, which prevents unnecessary transmission attempts when the AP and transmitter node are not facing each other.

When the AP turns into a new sector, it sends a Call-to-Action (CTA) packet to let client nodes know it is available to start a communication. Nodes that receive the CTA will answer with a Request-to-Send (RTS) packet if they have data to transmit. The AP will wait a certain wait time (T_{wait}) which is long enough to let the furthest node reply, and then decide on the next action. There are 3 possible scenarios:

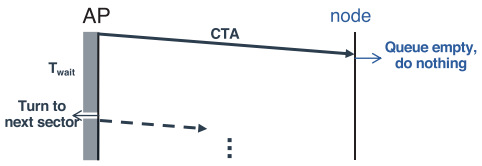

Fig. 2. Packet flow in the case of unanswered CTA.

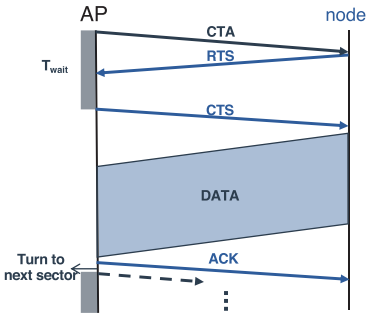

Fig. 3. Packet flow of a 3-way handshake, data transmission and acknowledgment between AP and one client node.

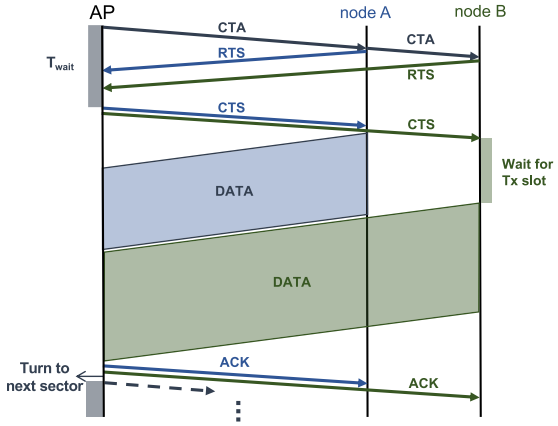

Fig. 4. Packet flow of a 3-way handshake, data transmission and acknowledgment for multiple active nodes in a sector.

- **0 RTS received:** If there are no client nodes in the sector, or they have an empty queue, the CTA will not trigger any response. After T_{wait}, the AP will skip this sector and turn to the next one, as in Fig. 2.
- **1 RTS received:** When a node has data to transmit, it will reply to the CTA with an RTS. If only one RTS has been received when T_{wait} expires, the AP will grant access to the channel with a Clear-to-Send (CTS) packet, completing the 3-way handshake. Upon the CTS reception, the node will send data (DATA), which will be acknowledged (ACK) if successfully received, as illustrated in Fig. 3. Only one DATA packet per node can be sent in a sector. If the node has more data in queue, it should be sent in subsequent cycles. This design choice limits the maximum sector time and reduces the delay for nodes waiting to transmit in other sectors, increasing the fairness of the proposed solution.
- **>1 RTS received.** When more than one RTS is received, all of them will be answered with a CTS each. The AP defines a transmission (Tx) slot for every node so that DATA packets do not collide, while making an efficient use of the channel. The timing information is included in the CTS. To reduce the propagation overhead, all CTS and ACK packets are grouped respectively in bursts. Again, only one DATA packet per node is allowed, the next packet should be sent in the following cycle. Fig. 4 shows the packet flow for the case of two nodes, and it can be extended for a higher number of nodes.

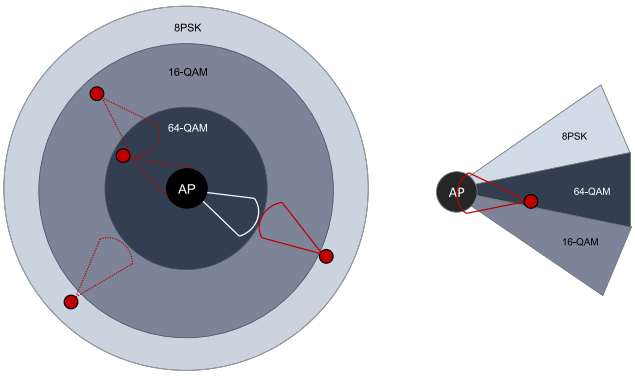

Fig. 5. Example of highest possible MCS depending on distance to the AP when using the primary sector (left), and MCS in the primary sector and adjacent sectors for a node close to the AP (right).

The performance of the protocol is governed by AP's cycle time, which is the time necessary to probe all sectors once and complete data transmissions, if any. Achieving a low cycle time is critical to reduce the latency of the protocol and increase the capacity.

Importantly, the sector time is adapted depending on the number of RTS received. An empty sector will be *skipped*, reducing cycle time, whereas, in busy sectors, the sector time will be extended to let all nodes complete the transmission of one DATA packet. This strategy greatly improves channel utilization compared to a fixed sector time approach.

Another benefit of the 3-way handshake is collision avoidance. DATA packets cannot collide, since exclusive Tx slots are defined; only RTS packets can collide. However, due to the very short transmission time of control packets, of few nanoseconds, RTS collisions are quite unlikely. Propagation delay (3.33 ns/m) multiplexes RTS packets in time, so nodes at different distances to the AP will never collide. Collisions can only occur between two nodes at a similar distance to the AP. To avoid systematic collisions, nodes wait a random backoff time of $[0, 10]$ ns before sending the RTS.

When collisions do occur, the Tx opportunity in the current AP cycle is lost, and nodes should retry in subsequent cycles. A random backoff mechanism will hold off the next retry to avoid colliding again. This is a count-based backoff with an initial life of $[0, 2^r]$, where r is the number of retries, and is decreased with every CTA received.

4.2. Adaptive MCS and white list

With the use of a 3-way handshake, new opportunities for optimization arise. We have designed an adaptive Modulation and Coding Scheme (MCS) mechanism that dynamically changes the modulation depending on signal power.

A higher order modulation encodes more information by using a more complex signal, but also requires a higher SNR to be decoded. With the pronounced path loss that affects THz signals, power at reception depends highly on distance (see Fig. 5). Control packets are always sent using the base MCS, which is simple enough for reliable communication with the furthest nodes. After the CTA-RTS exchange, the AP decides which MCS can a node use depending on the signal power received, and indicates it in the CTS. DATA is always transmitted using the highest possible modulation order, thus reducing DATA Tx time.

Since path loss is lower in short distances, nodes closer to the AP can use their primary sector and also adjacent sectors, even outside

of the 3 dB beamwidth. However, the gain is lower in adjacent sectors and a sub-optimal MCS would be used. We have implemented a sector's *white list* to avoid this situation. After a sounding phase, the AP creates a white list for every sector with the criteria of only allowing nodes to send data in their highest power sector. Thus, it ensures that the highest possible MCS is always used. The white list is checked before sending a CTS to a node. Another benefit of this strategy is that of guaranteeing that all nodes have one and only one DATA Tx opportunity per cycle, for maximum fairness.

4.3. 1-way variant

We also propose a variant of ADAPT with a 1-way handshake (ADAPT-1). The benefit of this approach is the reduction of overhead in the handshake. In this case, after receiving a CTA, nodes can directly send DATA.

The concept of adaptive sector time is still partially applied: the AP waits for T_{wait} and will turn to the next sector if it does not sense any DATA being received. If it does sense DATA, the AP waits until reception is finished and sends an ACK. The adaptive MCS strategy and sector's white list cannot be implemented as they require a 3-way handshake.

Communication with multiple nodes in a sector is not supported. In the case that two or more nodes send DATA, channel sensing is performed for collision avoidance, even though it is not reliable due to the deafness problem.

The comparison between the 3-way version (ADAPT-3) and ADAPT-1 will allow us to evaluate whether or not the benefits of a 3-way handshake outweigh the cost of introducing extra overhead.

4.4. A note on neighbor discovery

In the design presented we assume that all nodes know the position of the AP and are directionally listening towards it. However, we are aware that neighbor discovery is an open challenge in wireless directional networks. We have schemed an idea for a neighbor discovery protocol that would benefit from the design of ADAPT. This is meant to be developed in future work, but it is worth to present it in this article for completeness of the solution. The idea is to use CTA packets as AP beacon signals, merging discovery and communication in a single phase. Nodes would sweep all sectors listening for CTAs. If facing an AP, a node can expect to receive a CTA within the average cycle time, which, leveraging the very fast turning speed achieved in ADAPT, is in the order of few microseconds. The worst case scenario would be when all sectors have to be searched before finding the AP, which, in the setting studied, would be a very acceptable discovery time of under a millisecond.

5. Analytical model

In this section, we derive an analytical model of the 3-way ADAPT protocol for the scenario of a stable network and assuming no collisions, as the 3-way handshake greatly reduces collision probability. As we will see in Section 6.2, the model is accurate despite this simplification.

We consider nodes to be randomly distributed following a Poisson space distribution of rate λ_A nodes/m^2 around the central AP. For a range r, the total number of nodes is $N_{\text{nodes}} = \lambda_A \pi r^2$.

We model arrivals at every node as a Poisson process of rate λ packets/s, with an exponential distribution $\lambda e^{-\lambda t}$. It can be expressed in terms of the mean inter-arrival time as $\lambda = 1/T_{\text{ia}}$. Assuming no collisions, a node will have exactly one transmission opportunity at every cycle. Therefore, service rate μ depends only on cycle time (T_{cycle}), given by $\mu = 1/T_{\text{cycle}}$ packets/s. System load ρ is defined as the ratio between arrival and service rates, $\rho = \lambda/\mu$.

5.1. Cycle time

T_{cycle} has two components, a fixed time to sound all sectors and a variable term that depends on the number of data transmissions n in the cycle. It is expressed as

$$T_{\text{cycle}}(n) = N_{\text{sec}} T_{\text{wait}} + n\, T_{\text{tx}}. \tag{6}$$

T_{wait} must be long enough to let the furthest node reply with an RTS, and is defined as

$$T_{\text{wait}} = T_{\text{cta}} + \max(T_{\text{b/o}}) + T_{\text{rts}} + 2\max(T_{\text{prop}}), \tag{7}$$

where $T_{\text{b/o}}$ is a random backoff of $[0, 10]$ ns and T_{prop} is the one-way propagation time. T_{tx} accounts for the CTS-DATA-ACK exchange.

To formulate T_{tx}, we use an average T_{prop} and T_{data}. We acknowledge that T_{prop} depends on the distance from node to AP, different for each node, and the model should account for its distribution. However, we found the protocol to be accurately modeled using an average time (results in Section 6.2), while complexity is significantly reduced. Thus, T_{tx} is

$$T_{\text{tx}} = T_{\text{cts}} + T_{\text{data}} + T_{\text{ack}} + 2\,T_{\text{prop}}. \tag{8}$$

T_{cta}, T_{rts}, T_{cts}, T_{data} and T_{ack} represent transmission time for each type of packet. Each node can send either send zero or one packet in a cycle. The load ρ represents the probability that a node will have data to transmit. With a total of N_{nodes}, the probability of n transmissions in a cycle follows a binomial distribution given by

$$P_n = \binom{N_{\text{nodes}}}{n} (1-\rho)^{(N_{\text{nodes}}-n)} \rho^n, \tag{9}$$

with an expected value of $E[n] = N_{\text{nodes}}\,\rho$. Therefore, the average T_{cycle} is

$$T_{\text{cycle}} = N_{\text{sec}} T_{\text{wait}} + N_{\text{nodes}}\,\rho\, T_{\text{tx}}. \tag{10}$$

As for the distribution of T_{cycle}, we know that cycle time can only take a set of values corresponding to (6) for $n = 0, 1, 2, \ldots$. Therefore, the probability density function (PDF) of cycle time is not smooth, but shall be expressed as a set of Dirac delta functions placed at each of these time values, and weighted by the probability of n from (9), resulting in

$$f_{T_{\text{cycle}}}(t) = \sum_n P_n\, \delta(t - T_{\text{cycle}}(n)). \tag{11}$$

5.2. Stability condition

Stability is studied in terms of load ρ. The system requires that all nodes meet the condition $\rho < 1$ to be stable, meaning that arrival rate is lower than service rate. Otherwise, the number of packets in queue would be ever-growing, resulting in buffer overflow. Since all nodes have the same arrival and service rates, the system stability condition is given by

$$\rho = \frac{\lambda}{\mu} = \frac{T_{\text{cycle}}}{T_{\text{ia}}} < 1. \tag{12}$$

As T_{ia} is a fixed parameter, the system stability is defined by the T_{cycle} achieved. The faster the AP turns, the more transmission opportunities and more robust network. From (12) and (10), we can isolate ρ and express the stability condition as

$$\rho = \frac{N_{\text{sec}} T_{\text{wait}}}{T_{\text{ia}} - N_{\text{nodes}} T_{\text{tx}}} < 1. \tag{13}$$

5.3. Packet delay and throughput

To prevent buffer overflow and ensure stability the system needs $\rho < 1$, but for good network performance the load should be much lighter. In the packet delay and throughput analysis we will consider networks with $\rho \ll 1$.

We define packet delay T as the time from enqueue to reception of ACK. It is divided in three terms, expressed as

$$T = T_{\text{face}} + T_{\text{w}} + T_{\text{sector}}. \tag{14}$$

T_{face} is the time from arrival of the packet until the AP and node face. T_{w} is the wait time to send packets in queue. Lastly, T_{sector} is the sector time in which the packet is transmitted, from the moment CTA is sent until ACK is received.

For each packet, throughput is defined as $S = L/T$, where L is the payload length. For an accurate throughput estimate that captures the distribution of packet delay, we formulate the PDF of T, $f_T(t)$, and then compute throughput as

$$S = \int \frac{L}{t} f_T(t) dt. \tag{15}$$

T is a random variable formed by the sum of three independent random variables. Thus, its PDF is the convolution of the PDFs of its terms, expressed as

$$f_T(t) = f_{T_{\text{face}}}(t) * f_{T_{\text{w}}}(t) * f_{T_{\text{sector}}}(t). \tag{16}$$

Starting with T_{face}, the time from enqueue until the AP and node face each other is uniformly distributed between 0 and T_{cycle}, given by

$$T_{\text{face}} = U(0,1)\, T_{\text{cycle}}. \tag{17}$$

From (11) and (17), we can formulate the PDF of T_{face} as

$$f_{T_{\text{face}}}(t) = \sum_n P_n\, U[0, T_{\text{cycle}}(n)]. \tag{18}$$

For T_{w}, the wait time to send N_{w} packets, one cycle per packet, is

$$T_{\text{w}} = N_{\text{w}} T_{\text{cycle}}. \tag{19}$$

Considering that the service rate is much higher than arrival rate ($\rho \ll 1$), it is unlikely to find many packets in queue at the time of arrival. In our numerical analysis we will only consider the scenarios of $n_{\text{w}} = 0, 1$, with probabilities $P_{n_{\text{w}}}(0) = (1-\rho)$, $P_{n_{\text{w}}}(1) = \rho$, where n_{w} is the number of packets in queue. Hence, using (11), we can express the PDF of T_{w} as

$$f_{T_{\text{w}}}(t) = \sum_{n_{\text{w}}} P_{n_{\text{w}}}\, n_{\text{w}}\, f_{T_{\text{cycle}}}(t) = (1-\rho)\delta(t) + \rho\, f_{T_{\text{cycle}}}(t). \tag{20}$$

Lastly, T_{sector} corresponds to the time between CTA is sent until ACK is received, given by

$$T_{\text{sector}} = T_{\text{wait}} + 3\,T_{\text{prop}} + n_{\text{s}}(T_{\text{cts}} + T_{\text{data}} + T_{\text{ack}}). \tag{21}$$

It depends on the number of packets sent in the sector (n_{s}). For scenarios with $\rho \ll 1$ it is unlikely to have multiple transmissions in a sector. We will only consider $n_{\text{s}} = 1$. T_{data} is not fixed, it depends on the MCS chosen. Considering M possibilities, each modulation $m \in M$ has a probability P_m and DATA Tx time T^m_{data}. The resulting PDF is expressed as

$$f_{T_{\text{sector}}}(t) = \sum_m^M P_m\, \delta\big(t - (T_{\text{wait}} + 3T^m_{\text{prop}} + T_{\text{cts}} + T^m_{\text{data}} + T_{\text{ack}})\big). \tag{22}$$

At this point, we can derive $f_T(t)$ in (16) from (18), (20), (22). Then, we are able to estimate the system's throughput evaluating (15).

Table 2
Modulation schemes supported in 802.15.3d.

Modulation	Data rate [Gbps]	SNR_{th} [dB]	Range [m]
BPSK	52.4	10.6	48
QPSK	105.3	12.4	34
8PSK	157.4	17.6	18
16-QAM	210.2	19.2	15.4
64-QAM	315.4	25.4	7.5

6. Results

In this section, we investigate the performance of the protocol proposed, both the 3-way (ADAPT-3) and 1-way variant (ADAPT-1), in terms of throughput and packet discard rate. We compare them to the previous 1-way solution with fixed cycle time (1-way-2019), CSMA (0-way) and CSMA/CA (2-way). Cycle time and optimal packet size are also studied.

The protocols are implemented in the *ns-3* network simulator using TeraSim [11], an extension that models the peculiarities of the THz frequency-selective channel. TeraSim is available and free to download in the *ns-3* store. Extensive simulations are used to investigate the performance and validate the analytical model.

Each data point is the average of 10 simulations of different seed, with a duration of 10 ms each. This time duration is long enough to allow for hundreds of AP cycles, and short enough to consider a fixed scenario, as the impact of mobility is left for future work. Packet arrivals at every node follow a Poisson process of rate $\lambda = \frac{1}{T_{\text{ia}}}$, and a packet is discarded after 5 unsuccessful transmission attempts. More or longer simulations do not have a significant impact on the results, since a permanent state is reached after few microseconds of simulation.

6.1. Configuration

In our analysis, we use the physical layer proposed in the IEEE 802.15.3d standard for high data rate wireless networks [26]. We select a single carrier signal of $B = 69.12$ GHz, between $252.72 - 321.84$ GHz. In this window, the thermal noise for a temperature of 300 K is $N_T = -65.4$ dBm. Noise due to molecular absorption is very low at these frequencies and can be neglected. We assume a noise figure at reception of $N_F = 7$ dB. In the trade-off between gain and sectors, we have chosen a beamwidth of 12° that divides a cycle in 30 sectors and provides 24.57 dB of maximum gain. 802.15.3d supports modulations from BPSK to 64-QAM with a forward error correction (FEC) rate of 14/15. We calculate the SNR_{th} necessary to achieve a bit error rate (BER) of 10^{-6}. Transmission power is set to $P_t = 20$ dBm. After the effect of path loss and the gain of both antennas, the resulting power at reception P_r defines the range of communication. Reception will only be considered successful if $P_r/(N_F + N_T) > \text{SNR}_{\text{th}}$.

Table 2 shows the modulations and data rates supported in 802.15.3d, the SNR_{th} for the proposed BER and the maximum range for each modulation. We simulate a range of 18 m, so nodes will use either 8PSK, 16-QAM or 64-QAM, depending on P_r. Packet length is of 65 000 bytes. DATA Tx time at the highest modulation order of 64-QAM, with a data rate of 315.4 Gbps, is of 1.64 μs.

6.2. Throughput and discard rate

Figs. 6(a) and 6(b) show throughput against inter-arrival time and node density, respectively. With the AP covering a radius of 18 m, a node density of 0.05 nodes/m^2 represents 50 nodes.

We observe that ADAPT brings a notorious improvement, reaching throughput peaks of 120 Gbps, compared to the ∼10 Gbps of other solutions. The main reason for such improvement is the adaptive sector time mechanism, which greatly reduces cycle time and, thus, packet delay. As expected, when the network load is increased with a higher

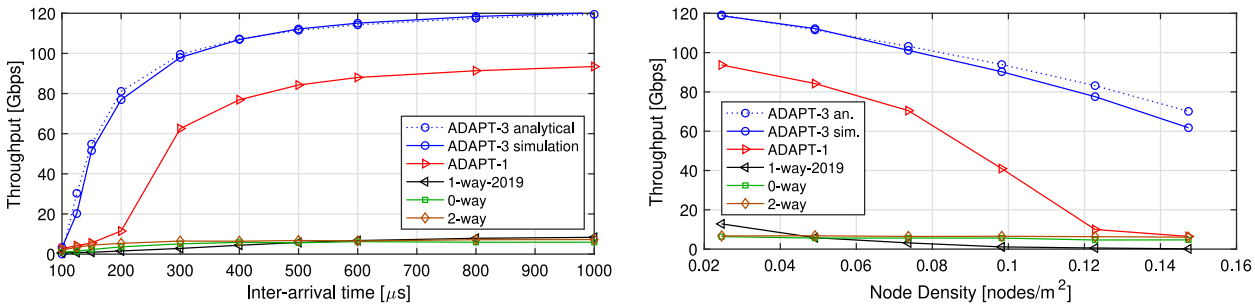

(a) Fixed node density at 0.05 nodes/m^2. (b) Fixed T_{ia} at 500 μs.

Fig. 6. Throughput simulation and analytical results for a range of 18 m.

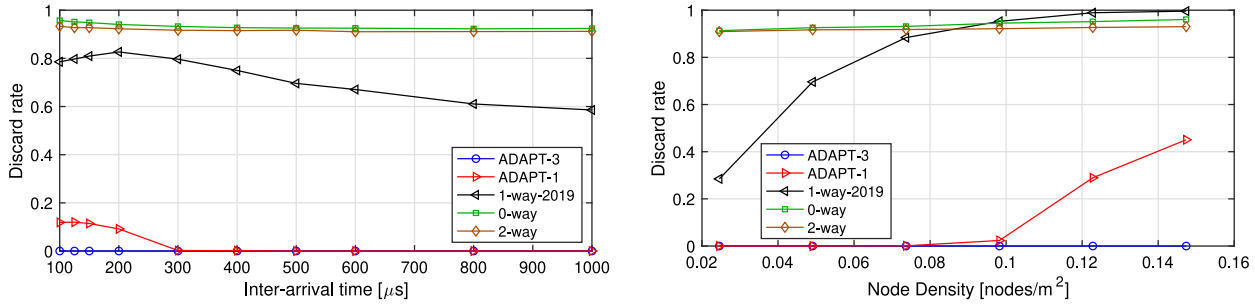

(a) Fixed node density at 0.05 nodes/m^2. (b) Fixed T_{ia} at 500 μs.

Fig. 7. Packet discard rate simulation results for a range of 18 m.

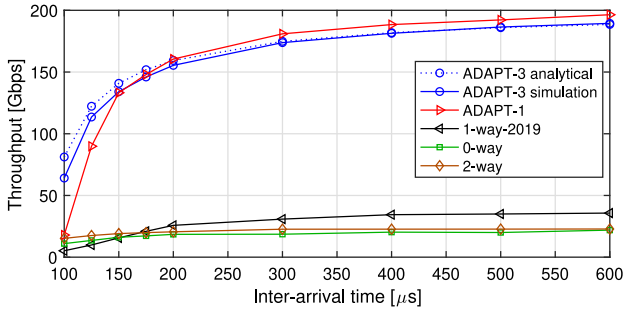

Fig. 8. Throughput simulation and analytical results for a range of 7.5 m. Fixed node density at 0.28 nodes/m^2.

node density or arrival rate, throughput decreases and the network eventually reaches an unstable point.

Also included in Fig. 6 is the analytical throughput for ADAPT-3. We validate the model by comparing analytical to simulation results. The analytical estimate is fairly accurate despite assuming no collisions, while collisions are taken into account in the simulations. Only in the scenarios with a higher network load, as collision probability rises, the analytical model slightly overestimates throughput.

Improvement is observed as well in packet discard rate, Figs. 7(a) and 7(b), as ADAPT-3 presents a null discard rate in all of the scenarios simulated. ADAPT-1 also reduces packet discards despite not having reliable collision avoidance, thanks to the faster turning speed. Transmitter-initiated handshakes prove not to be fit for a this network architecture. Since most transmission attempts will find the AP facing elsewhere, 0-way and 2-way protocols have a steadily high discard rate.

Comparing ADAPT-3 and ADAPT-1, we observe that the benefits of the 3-way handshake pay off and it reaches higher throughput rates than the 1-way, despite the larger overhead. This is due to the collision avoidance of the 3-way exchange and the adaptive MCS strategy.

To study protocol performance in smaller areas, a scenario of 7.5 m of range was also investigated. Fig. 8 shows throughput as a function of T_{ia} for 50 nodes. There are two major differences compared to the 18 m range. Firstly, all nodes will be able to use the highest modulation order of 64-QAM, nullifying the adaptive MCS strategy. ADAPT-3 loses its edge over ADAPT-1 and now both perform similarly. And secondly, with the shorter distance comes a lower propagation delay, which reduces cycle time and packet delay, and enables throughput rates up to 200 Gbps.

6.3. Cycle time

The AP's average cycle time is a key parameter that will define the performance of the protocol. Since nodes have one Tx opportunity per cycle, a faster turning speed means more frequent Tx opportunities, leading to less packet delay and a more stable network. Moreover, the cycle time also determines the latency of the system.

The improvement of ADAPT compared to the 1-way solution comes from the reduction of cycle time. Because of the adaptive sector time and MCS, T_{cycle} is also adaptive, unlike the previously fixed T_{cycle}. The minimum cycle time, in the case of zero data transmissions in a cycle, is the time to sound all sectors, $T_{cycle}^{min} = N_{sec}\, T_{wait}$. For the 18 m range, T_{cycle}^{min} is of 3.96 μs.

Overall, ADAPT-3 achieves a 20-fold reduction on the average T_{cycle} compared to 1-way-2019. Fig. 9(a) shows an inverse dependence between T_{cycle} and send rate, asymptotically approaching the minimum as the network load decreases. A similar behavior is observed in Fig. 9(b), as T_{cycle} rises when the network load is increased with a higher number of nodes. The distribution of nodes between the sectors does not affect significantly T_{cycle}. When the average cycle time is very close to the minimum, it effectively means that most sectors hold no DATA Tx and are skipped.

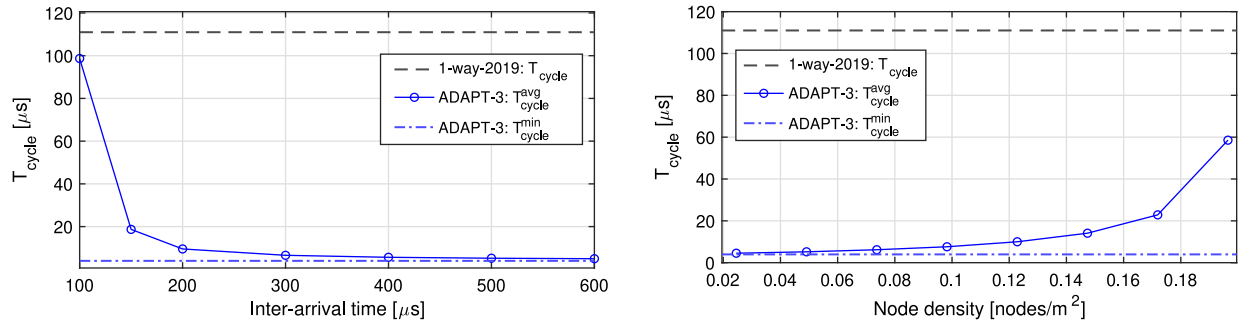

(a) Fixed node density at 0.05 nodes/m^2. (b) Fixed T_{ia} at 500 μs.

Fig. 9. Cycle time of 1-way-2019 and ADAPT-3 for a range of 18 m.

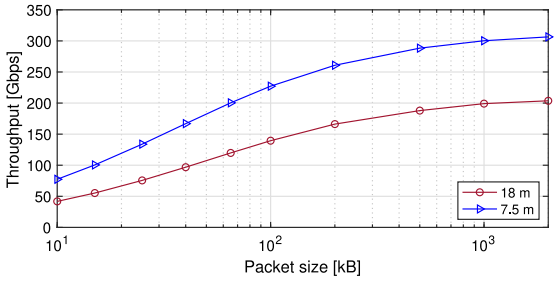

Fig. 10. Analytical throughput for ADAPT-3 as a function of packet size. Parameters: 50 nodes and 10 ms of T_{ia}.

6.4. Packet size

Very high speed networks in ultra-broadband communications open the door to the use of much larger payloads, as the faster data rates allow to transmit long packets in a very short time. Furthermore, in the network architecture presented, each Tx opportunity has a fixed delay cost, which is the waiting time until AP and node face each other. Sending more data in each Tx opportunity minimizes this cost. In 802.15.3d, payload size limits are set to a minimum of 2 kB and maximum of 2 MB. Our analysis was conducted with DATA payloads of 65 kB.

Fig. 10 shows the achievable throughput for packets between 2 kB–2 MB, estimated with the analytical model for a scenario of 50 nodes and T_{ia} of 10 ms. We can see how throughput as a function of packet size has a logarithmic growth and it approaches a superior limit set by the physical data rates. However, the use of long payloads also brings some concerns, such as error correction or the negative impact on latency. An optimal packet size, or the use of a dynamic payload, should be studied weighing up these concerns.

7. Future work

Link layer solutions for high-speed directional wireless networks are just starting to gain attention, and there are many open challenges still to be addressed.

In the design of ADAPT we have used a simplified scenario for a more clear presentation of the protocol. Future work can consider extending ADAPT for downlink communication, generalizing from 2-D to a 3-D space, or modeling node mobility. Another interesting question would be to include machine learning techniques, which could be used to learning the most active sectors or to adapt the beamwidth dynamically. Moreover, it would be of interest to study the use of multiple antennas in an AP, which could operate simultaneously by leveraging directional communication.

It will be important that future research investigates neighbor discovery solutions to overcome deafness, as it is a critical aspect for the feasibility of directional wireless networks. A possible path to explore is the idea presented in Section 4.4, which would work in synergy with ADAPT by leveraging the fast turning speed of the AP.

8. Conclusions

In this paper we present ADAPT, a MAC protocol for ultra-high-speed wireless directional networks in the THz band. It relies on a turning AP and receiver-initiated 3-way handshake for synchronization. An adaptive sector time mechanism improves channel utilization and reduces cycle time, while the 3-way handshake provides collision avoidance and optimization of the MCS. A variant of the protocol with a 1-way handshake is also studied. An analytical model that estimates the stability condition and packet delay is developed. The performance of the protocol is investigated analytically and with simulations in *ns-3*, using the physical layer parameters of IEEE 802.15.3d. Results show that ADAPT can achieve throughput in excess of 100 Gbps while reducing packet discard rate to virtually zero. Moreover, cycle time is greatly reduced, providing a lower latency. Despite the extra overhead, a 3-way handshake proves to generally perform better than a 1-way. Overall, the protocol presented improves existing MAC solutions for THz-band centralized networks.

Declaration of competing interest

The authors declare that they have no known competing financial interests or personal relationships that could have appeared to influence the work reported in this paper.

Acknowledgments

This work was supported in part by the US Air Force Research Laboratory Grant FA8750-20-1-0200 and the US National Science Foundation Grants CNS-2011411.

References

[1] I.F. Akyildiz, J.M. Jornet, C. Han, Terahertz band: Next frontier for wireless communications, Phys. Commun. 12 (2014) 16–32.

[2] A. Nikpaik, A.H.M. Shirazi, A. Nabavi, S. Mirabbasi, S. Shekhar, A 219-to-231 ghz frequency-multiplier-based vco with˜ 3% peak dc-to-rf efficiency in 65-nm cmos, IEEE J. Solid-State Circuits 53 (2) (2017) 389–403.

[3] E. Schlecht, J.V. Siles, C. Lee, R. Lin, B. Thomas, G. Chattopadhyay, I. Mehdi, Schottky diode based 1.2 thz receivers operating at room-temperature and below for planetary atmospheric sounding, IEEE Trans. Terahertz Sci. Technol. 4 (6) (2014) 661–669.

[4] J.V. Siles, K.B. Cooper, C. Lee, R.H. Lin, G. Chattopadhyay, I. Mehdi, A new generation of room-temperature frequency-multiplied sources with up to 10× higher output power in the 160-ghz–1.6-thz range, IEEE Trans. Terahertz Sci. Technol. 8 (6) (2018) 596–604.

[5] T. Nagatsuma, G. Ducournau, C.C. Renaud, Advances in terahertz communications accelerated by photonics, Nat. Photonics 10 (6) (2016) 371.

[6] Q. Lu, D. Wu, S. Sengupta, S. Slivken, M. Razeghi, Room temperature continuous wave, monolithic tunable thz sources based on highly efficient mid-infrared quantum cascade lasers, Sci. Rep. 6 (2016) 23595.
[7] K.S. Novoselov, V. Fal, L. Colombo, P. Gellert, M. Schwab, K. Kim, et al., A roadmap for graphene, nature 490 (7419) (2012) 192–200.
[8] A.C. Ferrari, F. Bonaccorso, V. Fal'Ko, K.S. Novoselov, S. Roche, P. Bøggild, S. Borini, F.H. Koppens, V. Palermo, N. Pugno, et al., Science and technology roadmap for graphene, related two-dimensional crystals, and hybrid systems, Nanoscale 7 (11) (2015) 4598–4810.
[9] M. Hasan, S. Arezoomandan, H. Condori, B. Sensale-Rodriguez, Graphene terahertz devices for communications applications, Nano Commun. Netw. 10 (2016) 68–78.
[10] S. Koenig, D. Lopez-Diaz, J. Antes, F. Boes, R. Henneberger, A. Leuther, A. Tessmann, R. Schmogrow, D. Hillerkuss, R. Palmer, et al., Wireless sub-thz communication system with high data rate, Nat. Photonics 7 (12) (2013) 977–981.
[11] Z. Hossain, Q. Xia, J.M. Jornet, Terasim: An ns-3 extension to simulate terahertz-band communication networks, Nano Commun. Netw. 17 (2018) 36–44.
[12] T. Nitsche, C. Cordeiro, A.B. Flores, E.W. Knightly, E. Perahia, J.C. Widmer, Ieee 802.11 ad: directional 60 ghz communication for multi-gigabit-per-second wi-fi, IEEE Commun. Mag. 52 (12) (2014) 132–141.
[13] Y. Ghasempour, C.R. da Silva, C. Cordeiro, E.W. Knightly, Ieee 802.11 ay: Next-generation 60 ghz communication for 100 gb/s wi-fi, IEEE Commun. Mag. 55 (12) (2017) 186–192.
[14] S. Ghafoor, N. Boujnah, M.H. Rehmani, A. Davy, Mac protocols for terahertz communication: A comprehensive survey, 2019, arXiv preprint arXiv:1904.11441.
[15] X.-W. Yao, J.M. Jornet, Tab-mac: Assisted beamforming mac protocol for terahertz communication networks, Nano Commun. Netw. 9 (2016) 36–42.
[16] W. Tong, C. Han, Mra-mac: A multi-radio assisted medium access control in terahertz communication networks, in: GLOBECOM 2017-2017 IEEE Global Communications Conference, IEEE, 2017, pp. 1–6.
[17] C. Han, W. Tong, X.-W. Yao, Ma-adm: A memory-assisted angular-division-multiplexing mac protocol in terahertz communication networks, Nano Commun. Netw. 13 (2017) 51–59.
[18] Q. Xia, Z. Hossain, M.J. Medley, J.M. Jornet, A link-layer synchronization and medium access control protocol for terahertz-band communication networks, IEEE Trans. Mob. Comput. (2019).
[19] Y. Ghasempour, R. Shrestha, A. Charous, E. Knightly, D.M. Mittleman, Single-shot link discovery for terahertz wireless networks, Nature Commun. 11 (1) (2020) 1–6.
[20] Q. Xia, J.M. Jornet, Expedited neighbor discovery in directional terahertz communication networks enhanced by antenna side-lobe information, IEEE Trans. Veh. Technol. 68 (8) (2019) 7804–7814.
[21] K. Sengupta, A. Hajimiri, A 0.28 thz power-generation and beam-steering array in cmos based on distributed active radiators, IEEE J. Solid-State Circuits 47 (12) (2012) 3013–3031.
[22] I.F. Akyildiz, J.M. Jornet, Realizing ultra-massive mimo (1024× 1024) communication in the (0.06–10) terahertz band, Nano Commun. Netw. 8 (2016) 46–54.
[23] A. Singh, M. Andrello, N. Thawdar, J.M. Jornet, Design and operation of a graphene-based plasmonic nano-antenna array for communication in the terahertz band, IEEE J. Sel. Areas Commun. (2020).
[24] J.M. Jornet, I.F. Akyildiz, Channel modeling and capacity analysis for electromagnetic wireless nanonetworks in the terahertz band, IEEE Trans. Wireless Commun. 10 (10) (2011) 3211–3221.
[25] C.A. Balanis, Antenna Theory: Analysis and Design, John wiley & sons, 2016.
[26] Ieee standard for high data rate wireless multi-media networks–amendment 2: 100 gb/s wireless switched point-to-point physical layer, in: IEEE Std 802.15.3d-2017 (Amendment to IEEE Std 802.15.3-2016 as Amended by IEEE Std 802.15.3e–2017), 2017, pp. 1–55.

Daniel Morales received the B.S. in Telecommunication Technologies and Services Engineering from the Universitat Politècnica de Catalunya (UPC), Barcelona, Spain, in 2020. From February 2020 to July 2020, he was a visiting researcher at Northeastern University, Boston, Massachusetts, where he joined the Ultra-broadband Nanonetworking laboratory and worked on link-layer solutions for wireless THz communications. Since August 2020, he is pursuing the M.S. in Information and Network Engineering at Kungliga Tekniska Högskolan (KTH), Stockholm, Sweden. His current interests include communication networks, signal processing and machine learning applications.

Josep Miquel Jornet received the Ph.D. degree in Electrical and Computer Engineering (ECE) from the Georgia Institute of Technology in 2013. Between 2013 and 2019, he was with the Department of Electrical Engineering at the University at Buffalo. Since August 2019, he has been an Associate Professor in the Department of ECE at Northeastern University. His research interests are in Terahertz-band communications and Wireless Nano-bio-communication Networks. He has co-authored more than 160 peer-reviewed scientific publications, one book, and has been granted 3 US patents. He is serving as the lead PI on multiple grants from U.S. federal agencies.